Journal of Visualized Experiments

How to Stabilize Protein: Stability Screens for Thermal Shift Assays and Nano Differential Scanning Fluorimetry in the Virus-X Project

--Manuscript Draft--

Article Type:	Invited Methods Article - JoVE Produced Video
Manuscript Number:	JoVE58666R3
Full Title:	How to Stabilize Protein: Stability Screens for Thermal Shift Assays and Nano Differential Scanning Fluorimetry in the Virus-X Project
Keywords:	DSF, nanoDSF, TSA, Protein Stability, Protein Purification, Protein Crystallography
Corresponding Author:	Ehmke Pohl UNITED KINGDOM
Corresponding Author's Institution:	
Corresponding Author E-Mail:	ehmke.pohl@durham.ac.uk
Order of Authors:	Ehmke Pohl
	Daniel Bruce
	Emily Cardew
	Stefanie Freitag-Pohl
Additional Information:	
Question	**Response**
Please indicate whether this article will be Standard Access or Open Access.	Open Access (US$4,200)
Please indicate the **city, state/province, and country** where this article will be **filmed**. Please do not use abbreviations.	Durham, UK

TITLE:

How to Stabilize Protein: Stability Screens for Thermal Shift Assays and Nano Differential Scanning Fluorimetry in the Virus-X Project

AUTHORS AND AFFILIATIONS:

Daniel Bruce[1], Emily Cardew[1], Stefanie Freitag-Pohl[2], Ehmke Pohl[1,2]

[1]Department of Biosciences, Durham University, Stockton Road, Durham, UK

[2]Department of Chemistry, Durham University, Lower Mountjoy, Stockton Road, Durham, UK

Corresponding Author:

Ehmke Pohl

ehmke.pohl@durham.ac.uk

Tel: +44 (0) 191 33 43619

Email Addresses of Co-authors:

Daniel Bruce (daniel.bruce@durham.ac.uk)

Emily Cardew (emily.cardew@durham.ac.uk)

Stefanie Freitag-Pohl (stefanie.freitag-pohl@durham.ac.uk)

KEYWORDS:

DSF, nanoDSF, TSA, protein stability, protein purification, protein crystallography

SUMMARY:

A protocol is presented to rapidly test the thermal stability of proteins in a variety of conditions through thermal shift assays and nano differential scanning fluorimetry. Buffer systems, salts and additives, together comprising three unique stability screens, are assayed with proteins to identify suitable buffers for functional and structural studies.

ABSTRACT:

The Horizon2020 Virus-X project was established in 2015 to explore the virosphere of selected extreme biotopes and discover novel viral proteins. To evaluate the potential biotechnical value of these proteins, the analysis of protein structures and functions is a central challenge in this program. The stability of protein sample is essential to provide meaningful assay results and increase the crystallizability of the targets. The thermal shift assay (TSA), a fluorescence-based technique, is established as a popular method for optimizing the conditions for protein stability in high-throughput. In TSAs, the employed fluorophores are extrinsic, environmentally-sensitive dyes. An alternative, similar technique is nano differential scanning fluorimetry (nanoDSF), which relies on protein native fluorescence. We present here a novel osmolyte screen, a 96-condition screen of organic additives designed to guide crystallization trials through preliminary TSA experiments. Together with previously-developed pH and salt screens, the set of three screens provides a comprehensive analysis of protein stability in a wide range of buffer systems and additives. The utility of the screens is demonstrated in the TSA and nanoDSF analysis of lysozyme and Protein X, a target protein of the Virus-X project.

INTRODUCTION:

Many biotechnologically-useful enzymes originate from viral sources, such as the tobacco etch virus (TEV) protease[1] and human rhinovirus type 3C (HRV 3C) protease[2]. The Horizon2020 Virus-X project (www.virus-x.eu) aims to determine the structures and functions of novel viral proteins of selected extreme microbial ecosystems including deep sea vents and Icelandic hot springs for potential biotechnological applications (**Figure 1**)[3]. The aim of this program is (a) to extend the range of the properties of known enzyme families and (b) to characterize novel enzymes of yet unknown function (Enzyme X). Crystallographic structure determination plays a pivotal role in target protein characterization, in particular in those cases where the protein sequences have evolved beyond recognition[4]. Protein stability is a key factor in the crystallization process; samples must be conformationally homogenous and structurally sound over a period of time to form high-quality, diffracting crystals. Furthermore, it is essential for activity assays that the proteins exist in their active conformation, which can also be facilitated by a favorable molecular environment.

Despite the development in the technology available to crystallographers, protein crystallization remains a time-consuming and labor-intensive empirical process[5]. Preliminary biophysical experiments to improve the protein stability in solution give clearly a better starting point for protein crystallization and consume usually only a comparatively small amount of protein sample[6-9]. The large number of target proteins to be studied in this project also necessitates scalable, high-throughput stability assays. One of the most popular methods for pre-crystallization biophysical characterization of the proteins is the thermal shift assay (also known as TSA or differential scanning fluorimetry, DSF)[10,11].

TSAs employ an environmentally-sensitive fluorescent dye to track the thermal denaturation of protein samples. Many commonly-used dyes have variable fluorescence activity depending on the polarity of their environment, often displaying a high fluorescence output in hydrophobic environments but undergoing rapid quenching in polar environments[12]. Proteins generally cause pronounced increases in dye fluorescence as their hydrophobic cores become exposed during denaturation, often followed by a decrease in dye fluorescence at very high temperatures as proteins begin to aggregate (**Figure 2**).

While a hydrophobicity-sensitive dye is often a good choice for a general-use TSA dye, it can be unsuitable for proteins with large, solvent-exposed hydrophobic regions, which often display detrimentally high background fluorescence. Fluorophores with alternative modes of action exist (see Discussion), but it may instead be desirable to track denaturation through intrinsic protein fluorescence with nanoDSF.

Tryptophan residues that are buried in nonpolar regions of a protein fluoresce with an emission maximum of 330 nm. As a protein sample unfolds and these residues become exposed to a polar solvent, their emission maximum undergoes a bathochromic shift to 350 nm[13]. nanoDSF exploits this shift in emission maximum to probe the unfolding of a protein sample without the need for extrinsic fluorophores[14].

Melt curves showing single denaturation steps can be analyzed by fitting data to a Boltzmann sigmoidal model. The temperature at the inflection point of the unfolding transition (T_m) is used as a quantitative measure of protein thermal stability and a benchmark to compare the favorability of different conditions.

Melt curves of the same protein in different conditions sometimes possess a degree of heterogeneity that can make a Boltzmann sigmoidal fitting unfeasible. To discern T_m values from data that deviates from the classic curve topology, numerical methods can be used such as those employed in NAMI, an open-source TSA data analysis program[11]. Alternative thermodynamic frameworks can also be used to analyze more complex curves with multiple denaturation steps, such as the ProteoPlex methodology[15].

The stability screens were designed for use in TSA and nanoDSF experiments to rapidly identify favorable conditions for a target protein (**Figure 3**, screen compositions are available in the supplementary information). Information gathered with the screens can be used at many stages of the crystallographic pipeline including: sample storage; purification, minimizing yield loss through protein unfolding during the purification process; assay design, reinforcing protein functionality in activity assays with thermally stabilizing buffers and finally crystallization, guiding rationally-designed crystallization trials.

Choosing a suitable buffer system basis for a protein sample is vital; incompatible pH values can lead to the deactivation or denaturation of a protein. However, the presence of co-crystallized buffer molecules resolved in a large number of X-ray crystal structures (**Table 1**) could also be indicative of a stabilizing effect that is separate to simple pH regulation and instead stems from the chemical features of the buffer molecule.

Formulated using several of Good's buffers[17-19] alongside other commonly biologically-compatible buffer systems, the pH screen is designed to deconvolute the chemical effect of a buffer molecule on protein stability from the actual pH of the resulting solution. By providing three pH values for each buffer system and incorporating pH value redundancy between different systems, the pH screen can identify both favorable pH values and favorable buffer systems for a target protein.

The salt screen contains commonly laboratory salts as well as chaotropes, chelants, heavy metals and reducing agents. The screen can give a general indication of the affinity of a protein sample to the environments with high ionic strengths, but each subgroup of the compounds can also provide information on the potential structure of a protein. For example, a chelant significantly destabilizing a protein could be indicative of important structural metals within the sample. If the sample is also strongly stabilized by a metal cation within the screen, this can provide a promising starting point for further structural experiments.

Osmolytes are soluble compounds that affect the osmotic properties of their environment. In nature, they can be used as "chemical chaperones", enforcing the folding of disordered proteins and stabilizing them, especially in stress conditions[20-22]. These characteristics make them

attractive additives in protein crystallography; usable as cryoprotectants during the crystal harvesting, mounting and storage processes[23]. Osmolytes' potential use also extends to the purification of proteins. A significant proportion of recombinant proteins expressed in *E. coli* can be insoluble and difficult to recover in the native state using standard purification methods. Osmolytes can be used to stabilize and salvage proteins from insoluble fractions, increasing purification yields[24].

The osmolyte screen was designed using established compounds present in Protein Data Bank entries[25] and the Dragon Explorer of Osmoprotection-Associated Pathways (DEOP)[26] database and iteratively optimized using standard proteins. The screen is built around eight subclasses of osmolyte: glycerol, sugars and polyols, non-detergent sulfobetaines (NDSBs), betaines and their analogues, organophosphates, dipeptides, amino acids and their derivatives and a final miscellaneous group. Each osmolyte is present in multiple concentrations based on its solubility and effective concentration ranges for comparison.

PROTOCOL:

1. Preparation of Protein Sample

1.1. Formulate the stability screens as 500 µL aliquots in 96-well blocks and seal for storage. Transfer 10 µL of each condition of a stability screen into the corresponding well of a 96-well plate using a multi-channel pipette to save time (**Figure 4A**).

1.2. Prepare 1 mL of an approximately 1 mg mL^{-1} protein solution in an appropriate buffer system. While the composition of an appropriate buffer varies with each protein sample, a good first buffer to try is 10 mM sodium phosphate with 100 mM NaCl, pH 7.2.

Note: Acceptable protein concentrations vary case-by-case, but concentration ranges of 0.5 – 5 mg mL^{-1} typically produce analyzable curves. Dilute buffers are recommended for use with the stability screens to avoid masking the effects of each condition. Typical buffer compositions are approximately 10 mM buffer with around 100 mM NaCl.

1.3. If performing a TSA experiment, add SYPRO Orange dye to the protein sample to a final concentration of 20x. Mix either by inversion or brief vortexing.

1.4. Transfer 10 µL of the protein solution into each well of the 96-well plate prepared in Step 1.1 (**Figure 4B**).

1.5. Seal and centrifuge the 96-well plate for 2 min at 600 x g to ensure the protein sample and screen component are mixed (**Figure 4C**).

1.6. Re-seal the stability screen deep well block and store the screen at 4 °C for up to 4 months. Store the salt screen in darkness, as some components are photosensitive.

1.7. If performing a nanoDSF experiment, continue to step 2. If performing a TSA experiment, skip to step 4.

2. Preparing a nanoDSF Experiment

2.1. Ensure that the equipment is clean, paying particular attention to any dust near the sample rack. If the system has a backscattering mirror, clean it using ethanol and a lint-free tissue.

2.2. Open the sample drawer by pressing the **Open Drawer** button. (**Figure 5A**).

2.3. Load the capillaries with approximately 10 µL from each well of the 96-well plate by touching one end of the capillary into the solution, then place them into the corresponding capillary holders of the sample rack (**Figure 5B**). Be careful not to contaminate the middle of the capillaries with fingerprints, *etc*., as this could interfere with fluorescence readings throughout the experiment.

2.4. Immobilize the capillaries with the magnetic sealing strip (**Figure 5C).**

3. Programming a nanoDSF Experiment

3.1. Launch a preliminary scan to detect the position and intensity of each capillary by pressing the **Start Discovery Scan** button in the **Discovery Scan** tab. Increase or decrease the incident excitation strength from an initial power of 10% until the peak of every capillary scan is between 4000-12000 units (**Figure 5D**).

3.2. To ensure the sample is folded and sufficiently concentrated, an initial melt scan with a steep temperature gradient is recommended. In the **Melting Scan** tab, program a melt scan by setting the **Temperature Slope** option to 7.0 °C min^{-1}, **Start Temperature** to 25 °C and **End Temperature** to 95 °C, then launch the nanoDSF experiment by pressing the **Start Melting** button. If the resulting melt curves do not show a detectable inflection point, consider concentrating the sample further or checking if the protein is folded properly.

3.3. Repeat steps 2.1-2.4 to prepare the samples for a full experiment.

3.4. In the **Melting Scan** tab, program a melt scan by setting the **Temperature Slope** option to 1.0 °C min^{-1}, **Start Temperature** to 25 °C and **End Temperature** to 95 °C, then launch the nanoDSF experiment by pressing the **Start Melting** button.

4. Performing a TSA Experiment

4.1. Open the sample drawer by firmly pressing the indent on the right-hand side of the drawer. Place the 96-well tray in the RT-PCR system with well A1 to the back-left (**Figure 4D**).

4.2. Click the **New Experiment** button to begin setting up a TSA experiment.

4.3. In the **Experiment Properties** tab, click the **Melt Curve** option when asked **What type of experiment do you want to set up**? and the **Other** option when asked **Which reagents do you want to use to detect the target sequence**?

4.4. In the **Plate Setup/ Define Targets and Samples** tab, enter a target name then set **Reporter** as **ROX** and **Quencher** as **None**.

4.5. In the **Plate Setup/ Assign Targets and Samples** tab, assign every well of the 96-well plate to the target name entered in the previous step. In the same tab, set **Select the dye to use as the passive reference** as **None**.

4.6. In the **Run Method** tab, delete steps until there is a total of three. Set the first step to 25.0 °C, ramp rate 100%, time 00:05; the second step to 95.0 °C, ramp rate 1%, time 01:00; the third step to 95.0 °C, ramp rate 100%, time 00:05. Choose to collect data using the **Collect Data** dropdown menu or by pressing the **Data Collection** icon (**Figure 6**).

4.7. Set the **Reaction Volume Per Well** to 20 µL.

4.8. Press the **Start Run** button to begin the TSA experiment.

5. Data Analysis

5.1. Choose a wavelength to plot a melt curve with. For nanoDSF experiments, the ratio of fluorescence intensities at 330 nm and 350 nm (corresponding to tryptophan in nonpolar and polar environments, respectively)[13] is commonly used. For most TSAs, the dye emission maximum is suitable for melt curve plotting (the emission maximum of SYPRO Orange is 569 nm)[12].

5.2. Calculate the T_m values of each condition by determining the inflection point(s) of each melt curve. Most nanoDSF systems automatically calculate T_m values by numerical differentiation of melt curves after data acquisition. If the software used does not automatically calculate T_m values, free, alternative GUI-driven software such as NAMI[11] can automate data analysis and downstream processing, giving the option to produce a heatmap summarizing T_m values for the entire 96-well experiment (the accompanying reference provides guidance and resources for data processing with NAMI).

5.3. Compare T_m values of all conditions surveyed. The stability screens contain two wells in each screen (A1 and A2) that contain only water. Taking the water-only values as a benchmark allows calculation of ΔT_m values, addressing systematic errors and allowing easy comparison of stabilizing effects. Higher T_m values indicate thermally stabilizing conditions which are recommended for downstream use. Promising conditions often show a concentration dependence in their stabilization.

REPRESENTATIVE RESULTS:

Lysozyme was assayed with the stability screens and Protein X, a target protein in the Virus-X project, was assayed with the osmolyte screen. Both proteins generally produced melt curves with clearly-defined denaturation transitions in both TSA and nanoDSF experiments (see accompanying figures for representative curves). In a few cases where the samples that did not produce interpretable curves with a defined denaturation transition were interpreted as denatured and not included in T_m comparisons.

Figure 7 shows sample results from the salt screen, exemplifying the thermally-stabilising properties of ammonium chloride towards lysozyme. Concentration dependencies such as that shown above are often indicative of promising conditions, but it can be useful to compare the results of increasing ion concentration with several different salts to see if thermal stabilisation generally arises from an increase in buffer ionic strength or if the presence of specific ions confers additional stability.

Comparison of T_m values of lysozyme with the pH screen (**Figure 8**) reveals two pieces of information. Firstly, there is a general trend of increasing stability with decreasing pH values. Secondly, the range of T_m values obtained using different buffer systems with identical pH values can be significant.

Data in **Figure 8** suggests that the agreement between TSA and nanoDSF in this experiment is generally good, but nanoDSF shows a tendency to identify slightly higher T_m values and slightly larger T_m shifts than TSA. However, some wells with pH values above 8.5 show large discrepancies between T_m values obtained from TSA and nanoDSF. Differences could potentially be attributed to the denaturation mechanism of the protein at different pH values; for example, a hydrophobicity-sensitive dye could give a comparatively low T_m reading if hydrophobic regions of a protein become exposed to solvent significantly faster than the environment of tryptophan residues changes in polarity.

Figure 9 shows a heatmap of T_m values obtained with lysozyme using the osmolyte screen. Conditions with the highest T_m increases compared to the control wells (wells A1 and A2, containing deionized water) are colored dark blue. Especially stabilizing conditions identified in **Figure 9** include glycerol, 1 M D-sorbitol, 100 mM hypotaurine and 10 mM Ala-Gly (wells A4-A6, A9, E7 and F8, respectively).

Figure 10 shows a heatmap of T_m values obtained with Protein X. TSA and nanoDSF experiments with the Osmolyte screen reveal that the majority of osmolytes tested give either a minor increase in T_m (within 1 °C) or have a detrimental effect on Protein X's stability. In particular, dipicolinic acid at a concentration of 10 mM (well D1) appears to denature the sample at room temperature. The TSA and nanoDSF results quickly identify dipicolinic acid as an incompatible additive for Protein X which should be avoided when working with the protein. Nevertheless, high concentrations of D-sorbitol and arabinose (wells A9 and B9, both at 1 M) as well as glycerol and TMAO (wells A4-A6 and E1, respectively) were identified as thermally-stabilizing.

For lysozyme, combinations of conditions yielding the highest T_m values from each stability screen were tested to probe for a synergistic combined effect. **Figure 11** shows a general increase in T_m values as more components of the buffer system (pH, salt and osmolyte) are added. In the case of MES, ammonium sulphate and D-sorbitol, a T_m increase as large as 10 °C can be observed when all components are present compared to MES alone. **Figure 11** shows that a noticeable synergistic effect can occur when individual components of a buffer are optimized and combined with the stability screens.

On a more general note, **Figure 11** also illustrates the magnitude of ΔT_m values that can be observed in TSA and nanoDSF experiments. The magnitude of ΔT_m achievable varies significantly based on the protein system, but any ΔT_m value around and above 5 °C is often indicative of a beneficial stabilizing effect.

FIGURE AND TABLE LEGENDS:

Figure 1: **Bioprospecting.** Sample collection from an extreme environment in the Virus-X Project.

Figure 2: TSA schematic. Annotated example of a typical melt curve obtained from a TSA experiment. This curve is characteristic of classic "two-state" protein unfolding, where the sample population transitions from folded to denatured without detectable partially-folded intermediates.

Figure 3: Stability screens workflow. Standard workflow of buffer optimization using the stability screens.

Figure 4: Workflow of a standard TSA experiment with the stability screens. From left to right: (A) Pipetting aliquots of the stability screens into a 96-well plate. (B) Pipetting protein sample with fluorescent dye into the plate. (C) Sealing the plate before centrifugation. (D) Placing the plate into an RT-PCR system.

Figure 5: Workflow of a standard nanoDSF experiment. (A) Opening the capillary loading rack. (B) Loading the capillaries into the rack. (C) Immobilizing the capillaries with the magnetic sealing strip. (D) Programming an experiment.

Figure 6: User interface for the RT-PCR system. A TSA experiment has been programmed.

Figure 7: Salt screen sample data. (A) Ratio of fluorescence intensities at 350 nm vs 330 nm for a label-free nanoDSF experiment with lysozyme. Samples correspond to the wells C7-C12 of the salt screen (1.5 M – 0.2 M ammonium chloride). Calculated T_m values for each condition are superimposed on the plot. (B) Summary of T_m values calculated from the data presented in **Figure 7A**. (C) Fluorescence intensities at 590 nm for a TSA experiment using lysozyme with a hydrophobicity-sensitive reporter dye. Like **Figure 7A**, the samples correspond to the wells C7-C12 of the salt screen. Calculated T_m values are superimposed on the graph. (D) Summary of T_m values calculated from data present in **Figure 7C**.

Figure 8: pH screen sample data. Summary of T_m shifts obtained with lysozyme and the pH screen. Each point represents an independent condition; points at the same pH value are of different buffer systems at the same pH. T_m shifts are calculated relative to a control T_m of 68.0 °C for TSA experiments and 71.9 °C for nanoDSF experiments.

Figure 9: Osmolyte screen sample data (lysozyme). Summary of T_m values obtained from a label-free nanoDSF experiment with lysozyme and each well of the osmolyte screen. T_m values (in °C) are compared to the wells A1 and A2 which contain water as a control. A heatmap was generated based on ΔT_m values compared (blue denotes a T_m increase and red a T_m decrease).

Figure 10: Osmolyte screen sample data (Protein X). (A) Summary of T_m values obtained from a label-free nanoDSF experiment with Protein X and the osmolyte screen. T_m values are compared to wells A1 and A2 which contain water as a control. A heatmap was generated based on ΔT_m values compared (blue denotes a T_m increase and red a T_m decrease). (B) nanoDSF curves obtained from well A9 (1 M D-sorbitol, a stabilizing condition) and D1 (10 mM dipicolinic acid, a destabilizing condition).

Figure 11: Buffer optimization effect on T_m. TSA T_m values of lysozyme combined with the conditions of each screen that afforded the largest increase in T_m. 100 mM acetic acid, pH 4.2, and 100 mM MES, pH 5.6, were chosen as the buffer systems, alongside 1.5 M ammonium sulphate as the salt. Osmolyte concentrations were identical to those found in the osmolyte screen: 10 mM Ala-Gly, 1 M D-sorbitol, 50 mM L-lysine and 100 mM hypotaurine. Error bars represent the standard deviation of six replicates.

Table 1: Summary of buffer molecule co-crystallization frequency in Protein Data Bank (PDB) entries. Data obtained through PDBsum[16] from a total of 144,868 entries (correct as of 12-5-18).

Supplementary File. See attached file: "Supplementary_Information.docx" and Supplementary Table 1-3 files.

DISCUSSION:

Critical aspects within the protocol include the centrifugation step and proper sealing of the 96-well plate for TSA experiments (step 1.5). Centrifugation ensures that the protein sample and screen condition come into contact and mix. Additionally, if an unsealed plate is used for a TSA experiment, there is a significant risk of solvent evaporating throughout the experiment, causing an increase in sample concentration and increasing the chance of premature protein aggregation.

TSAs and nanoDSF are amenable to a wide range of protein samples; the vast majority of samples can produce interpretable melt curves with a hydrophobicity-based reporter dye or through dye-free nanoDSF. If standard fluorescence sources are not suitable for your protein, the simplest modification to the protocol that could be explored is the choice of fluorophore. Several alternative dyes could be suitable for TSA experiments. Examples include N-[4-(7-diethylamino-4-methyl-3-coumarinyl)phenyl]maleimide (CPM), a compound that fluoresces after reacting with a thiol[27], and 4-(dicyanovinyl)julolidine (DCVJ), a compound that varies its fluorescence based on

the rigidity of its environment, increasing its fluorescence as a protein sample unfolds[28,29] (the latter dye often requires high concentrations of sample).

Alternative methods of melt curve analysis are available if T_m is not automatically calculated by the instrument software. If data is homogenous and only one denaturation step is apparent in the melt curves, a truncated dataset can be fitted to a Boltzmann sigmoid with the following equation:

$$F = F_{min} + \frac{F_{max} - F_{min}}{1 + \exp\left(\frac{T_m - T}{C}\right)}$$

Where F is the fluorescence intensity at temperature T, F_{min} and F_{max} are the fluorescence intensities before and after the denaturation transition, respectively, T_m is the midpoint temperature of the denaturation transition and C is the slope at T_m. While this method works well for simple two-step denaturation processes, it is unsuitable for complex melt curves with multiple transitions.

One of the major advantages of TSA is its accessibility; TSA experiments can be performed in any RT-PCR system with filters at suitable wavelengths for the fluorescence dye employed. This coupled with the low cost of consumables, ease of operation and relatively low amount of protein needed, make TSA a valuable technique for a wide range of project scales, both in industry and academia.

As well as indicating favorable buffer conditions, the screens contain some wells that may give clues to the presence of structural metals within a sample protein. Wells that may be of particular interest in the salt screen are G6 and G7, which contain 5 mM EDTA and 5 mM EGTA, respectively. Significant thermal destabilization in these wells may be indicative of important metal ions in the protein that are sequestered by the chelants. Compounds within the osmolyte screen can also potentially provide clues to the function of a protein. Many of the compounds in the screen belong to classes of molecule that are common substrates of enzymes. For example, the general stabilization afforded by saccharides (present in wells A11-B10) for lysozyme could be attributed to their structural similarity to established substrates of the enzyme, N-acetylglucosamine oligomers[30].

The TSA and nanoDSF protocols outlined above can also be adapted to study protein-ligand interactions. Ligands that bind specifically to a protein can increase its thermal stability by introducing new interactions within the complex. A dose-dependent positive shift in protein T_m is a promising sign of a successful protein-ligand interaction. The speed, throughput and low cost of screening compound libraries with TSAs has made it a very popular method in early-stage drug discovery.

Optimizing the buffer conditions of target proteins and their ligand complexes can be essential for a project's success, as many literature examples demonstrate[31-34]. With a typical assay taking

under 2 h including setup time, TSAs and nanoDSF coupled with stability screens represent a fast, inexpensive technique for buffer optimizations.

ACKNOWLEDGMENTS:

This project has received funding from the European Research Council (ERC) under the European Union's Horizon 2020 research and innovation programme (grant agreement n° 685778). This work was supported by the Biotechnology and Biological Sciences Research Council (BBSRC, grant numbers BB/M011186/1, BB/J014516/1). DB thanks the BBSRC Doctoral Training Partnership Newcastle-Liverpool-Durham for a studentship and Durham University Department of Biosciences for contributing toward the funding this work. We thank Ian Edwards for his help and the Durham University Department of Chemistry Mass Spectrometry department for their instrumental analysis of Protein X. We are grateful to Arnthor Ævarsson for his work with the Virus-X project, and thanks also to Claire Hatty and NanoTemper GmbH for lending and assisting with the Prometheus NT.48 system for this project. Finally, thank you to Frances Gawthrop and Tozer Seeds for their support as part of the BBSRC iCASE award.

DISCLOSURES:

The authors have nothing to disclose.

REFERENCES:

1. Kapust, R.B., Waugh, D.S. Controlled intracellular processing of fusion proteins by TEV protease. *Protein Expression and Purification.* **19** (2), 312-318 (2000).
2. Cordingley, M. G., Register, R. B., Callahan, P. L., Garsky, V. M., & Colonno, R. J. Cleavage of small peptides in vitro by human rhinovirus 14 3C protease expressed in *Escherichia coli. Journal of Virology*, **63** (12), 5037-5045 (1989).
3. Hjorleifsdottir, S., Aevarsson, A., Hreggvidsson, G.O., Fridjonsson, O.H., Kristjansson, J.K. Isolation, growth and genome of the Rhodothermus RM378 thermophilic bacteriophage. *Extremophiles*. **18** (2), 261–270 (2014).
4. Alva, V., Nam, S.Z., Söding, J., Lupas, A.N. The MPI bioinformatics Toolkit as an integrative platform for advanced protein sequence and structure analysis. *Nucleic Acids Research*. **44** (W1), W410–W415 (2016).
5. McPherson, A. Protein Crystallization. *Methods in molecular biology (Clifton, N.J.).* **1607**, 17–50 (2017).
6. Ericsson, U.B., Hallberg, B.M., DeTitta, G.T., Dekker, N., Nordlund, P. Thermofluor-based high-throughput stability optimization of proteins for structural studies. *Analytical Biochemistry.* **357** (2), 289–298 (2006).
7. Reinhard, L., Mayerhofer, H., Geerlof, A., Mueller-Dieckmann, J., Weiss, M.S., IUCr Optimization of protein buffer cocktails using Thermofluor. *Acta Crystallographica Section F Structural Biology and Crystallization Communications.* **69** (2), 209–214 (2013).
8. Boivin, S., Kozak, S., Meijers, R. Optimization of protein purification and characterization using Thermofluor screens. *Protein Expression and Purification.* **91** (2), 192–206 (2013).
9. Kozak, S., Lercher, L., Karanth, M.N., Meijers, R., Carlomagno, T., Boivin, S. Optimization of protein samples for NMR using thermal shift assays. *Journal of Biomolecular NMR.* **64** (4), 281–289 (2016).

10. Semisotnov, G. V, Rodionova, N.A., Razgulyaev, O.I., Uversky, V.N., Gripas', A.F., Gilmanshin, R.I. Study of the "molten globule" intermediate state in protein folding by a hydrophobic fluorescent probe. *Biopolymers.* **31** (1), 119–28 (1991).
11. Grøftehauge, M.K., Hajizadeh, N.R., Swann, M.J., Pohl, E. Protein-ligand interactions investigated by thermal shift assays (TSA) and dual polarization interferometry (DPI). *Acta Crystallographica Section D: Biological Crystallography.* **71**, 36–44 (2015).
12. Steinberg, T.H., Jones, L.J., Haugland, R.P., Singer, V.L. SYPRO Orange and SYPRO Red Protein Gel Stains: One-Step Fluorescent Staining of Denaturing Gels for Detection of Nanogram Levels of Protein. *Analytical biochemistry.* **239**, 223–237 (1996).
13. Burstein, E.A., Vedenkina, N.S., Ivkova, M.N. Fluorescence and the location of tryptophan residues in protein molecules. *Photochemistry and Photobiology.* **18** (4), 263–279 (1973).
14. Haffke, M., Rummel, G., Boivineau, J., Münch, A., Jaakola, V.-P. nanoDSF: label-free thermal unfolding assay of G-protein-coupled receptors for compound screening and buffer composition optimization. *Application Note NT-PR-008* (2016).
15. Chari, A. et al. ProteoPlex: stability optimization of macromolecular complexes by sparsematrix screening of chemical space. *Nature Methods.* **12** (9), 859–865 (2015).
16. Laskowski, R.A. PDBsum: summaries and analyses of PDB structures. *Nucleic Acids Research.* **29** (1), 221–222 (2001).
17. Good, N.E., Winget, G.D., Winter, W., Connolly, T.N., Izawa, S., Singh, R.M. Hydrogen ion buffers for biological research. *Biochemistry.* **5** (2), 467–77 (1966).
18. Good, N.E., Izawa, S. Hydrogen ion buffers. *Methods in enzymology.* **24**, 53–68 (1972).
19. Ferguson, W.J. et al. Hydrogen ion buffers for biological research. *Analytical biochemistry.* **104** (2), 300–10 (1980).
20. Welch, W.J., Brown, C.R. Influence of molecular and chemical chaperones on protein folding. *Cell stress & chaperones.* **1** (2), 109–15 (1996).
21. Diamant, S., Eliahu, N., Rosenthal, D., Goloubinoff, P. Chemical chaperones regulate molecular chaperones in vitro and in cells under combined salt and heat stresses. *The Journal of biological chemistry.* **276** (43), 39586–91 (2001).
22. Yancey, P.H. Organic osmolytes as compatible, metabolic and counteracting cytoprotectants in high osmolarity and other stresses. *Journal of Experimental Biology.* **208** (15), 2819–2830 (2005).
23. Garman, E.F., Owen, R.L. Cryocooling and radiation damage in macromolecular crystallography. *Acta Crystallographica Section D Biological Crystallography.* **62** (1), 32–47 (2006).
24. de Marco, A., Vigh, L., Diamant, S., Goloubinoff, P. Native folding of aggregation-prone recombinant proteins in Escherichia coli by osmolytes, plasmid- or benzyl alcohol–overexpressed molecular chaperones. *Cell Stress & Chaperones.* **10** (4), 329 (2005).
25. Berman, H.M. et al. The protein data bank. *Nucleic acids research.* **28** (1), 235–242, (2000).
26. Bougouffa, S., Radovanovic, A., Essack, M., Bajic, V.B. DEOP: A database on osmoprotectants and associated pathways. *Database.* 2014 (0), 1–13 (2014).
27. Alexandrov, A.I., Mileni, M., Chien, E.Y.T., Hanson, M.A., Stevens, R.C. Microscale Fluorescent Thermal Stability Assay for Membrane Proteins. *Structure.* **16** (3), 351–359 (2008).

28. Kung, C.E., Reed, J.K. Fluorescent molecular rotors: a new class of probes for tubulin structure and assembly. *Biochemistry.* **28** (16), 6678–8 (1989).
29. Iio, T., Itakura, M., Takahashi, S., Sawada, S. 9-(Dicyanovinyl)julolidine binding to bovine brain calmodulin. *Journal of biochemistry.* **109** (4), 499–502 (1991).
30. Veros, C.T., Oldham, N.J. Quantitative determination of lysozyme-ligand binding in the solution and gas phases by electrospray ionisation mass spectrometry. *Rapid Communications in Mass Spectrometry.* **21** (21), 3505–3510 (2007).
31. Kean, J., Cleverley, R.M., O'Ryan, L., Ford, R.C., Prince, S.M., Derrick, J.P. Characterization of a CorA Mg^{2+} transport channel from *Methanococcus jannaschii* using a Thermofluor-based stability assay. *Molecular membrane biology*, **25** (8), 653-661 (2008).
32. Geders, T.W., Gustafson, K., Finzel, B.C. Use of differential scanning fluorimetry to optimize the purification and crystallization of PLP-dependent enzymes. *Acta Crystallographica Section F*, **68** (5), 596-600 (2012).
33. Morgan, H.P., Zhong, W., McNae, I.W., Michels, P.A., Fothergill-Gilmore, L.A., Walkinshaw, M.D. Structures of pyruvate kinases display evolutionarily divergent allosteric strategies. *Royal Society open science*, **1** (140120), (2014).
34. Moretti, A., Li, J., Donini, S., Sobol, R.W., Rizzi, M., Garavaglia, S. Crystal structure of human aldehyde dehydrogenase 1A3 complexed with NAD+ and retinoic acid. *Scientific reports*, **6** (35710), (2016)

Figure

Click here to access/download;Figure;Figure_1.JPG

Figure

Click here to access/download;Figure;Figure_2.png

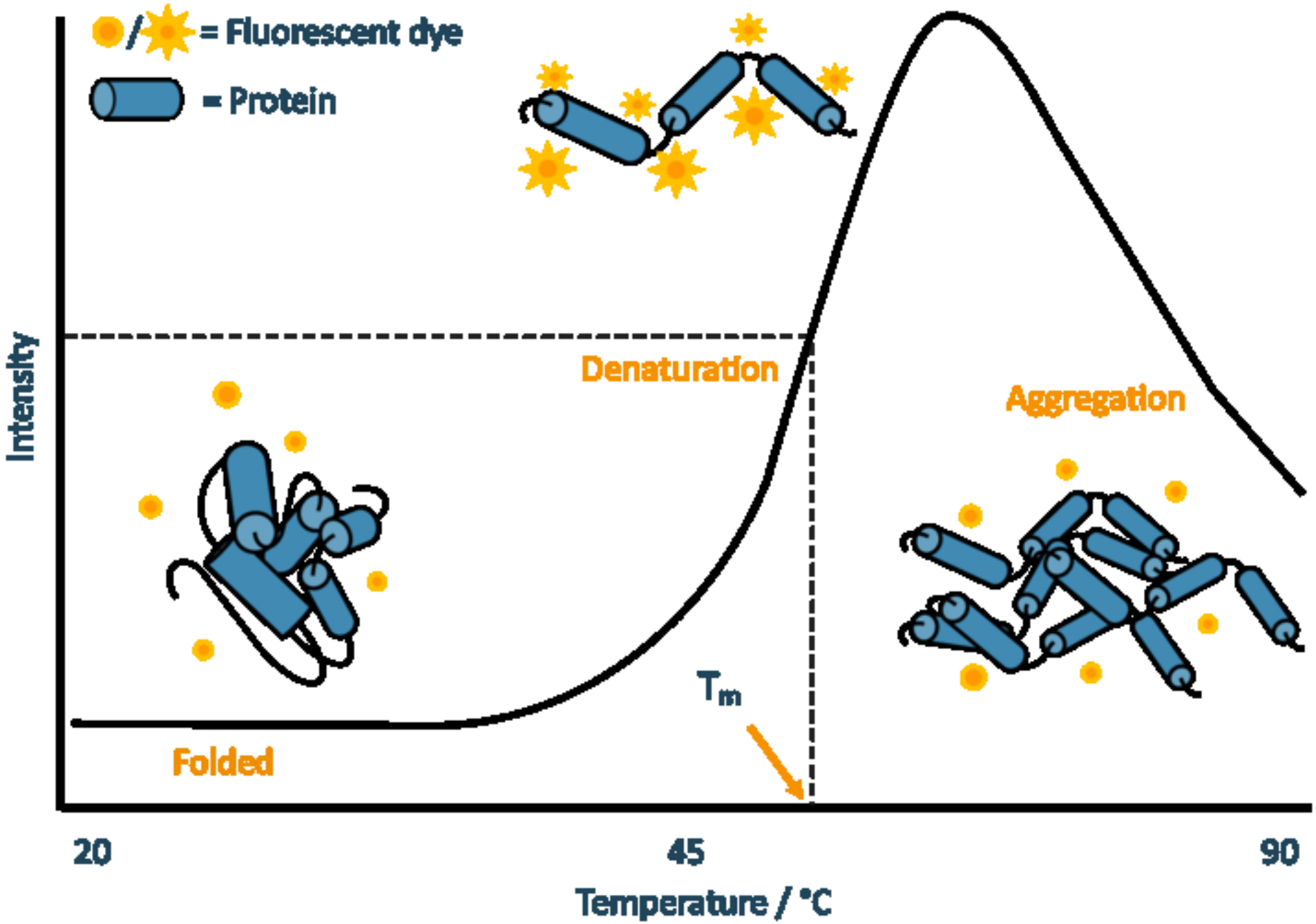

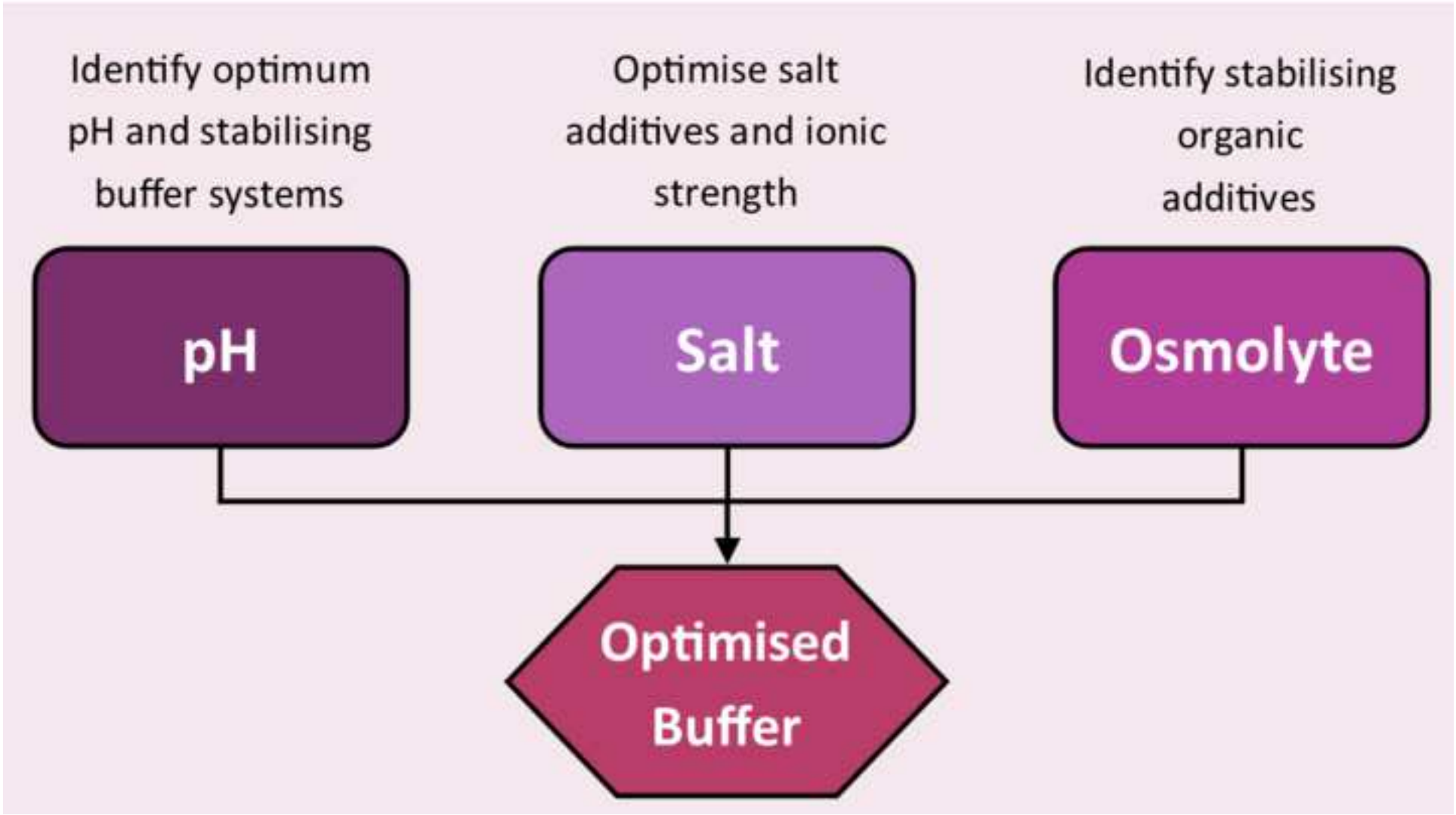

Figure

Click here to access/download;Figure;Figure_4.jpg

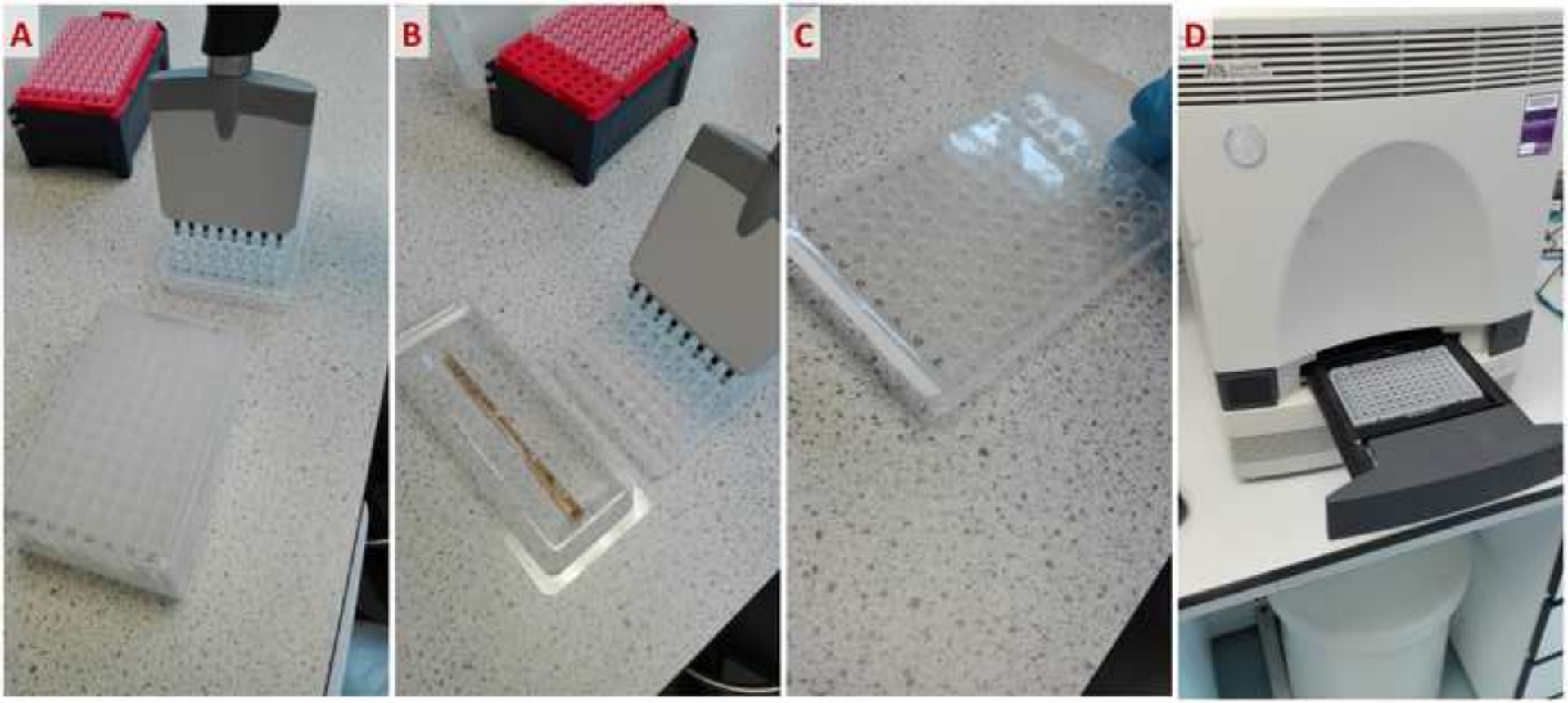

Figure

Click here to access/download;Figure;Figure_5.jpg

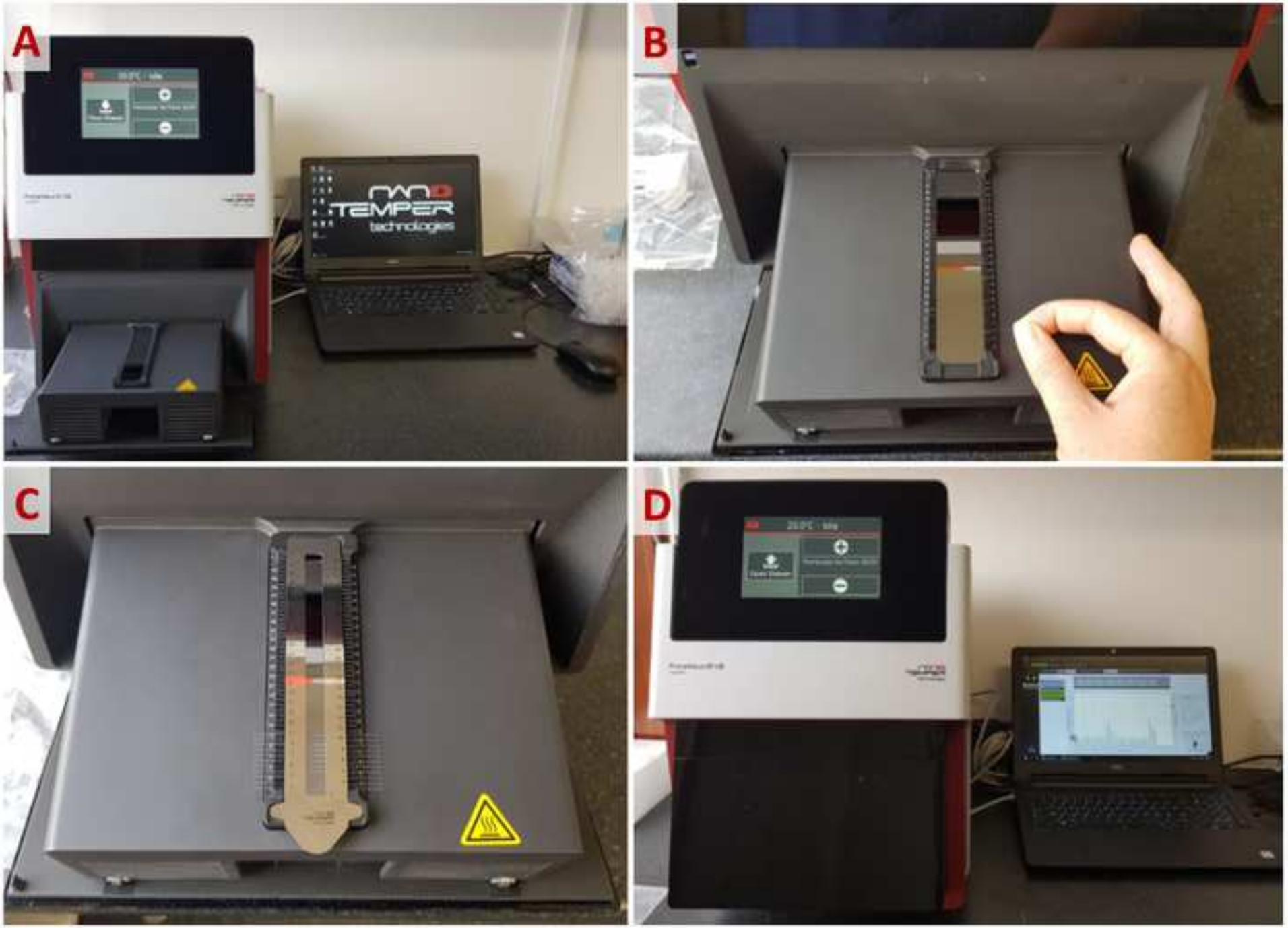

Figure

Click here to access/download;Figure;Figure_6.png

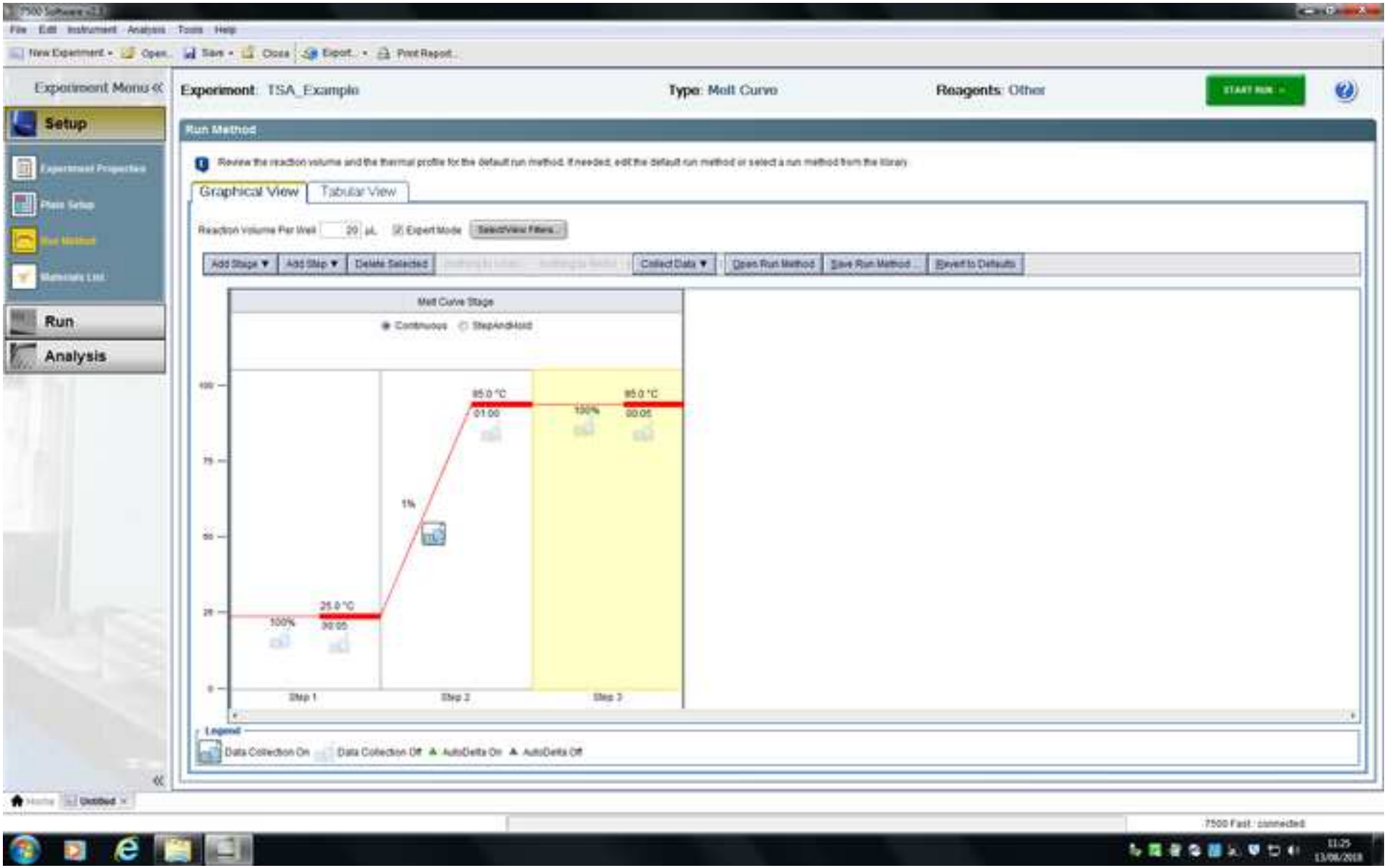

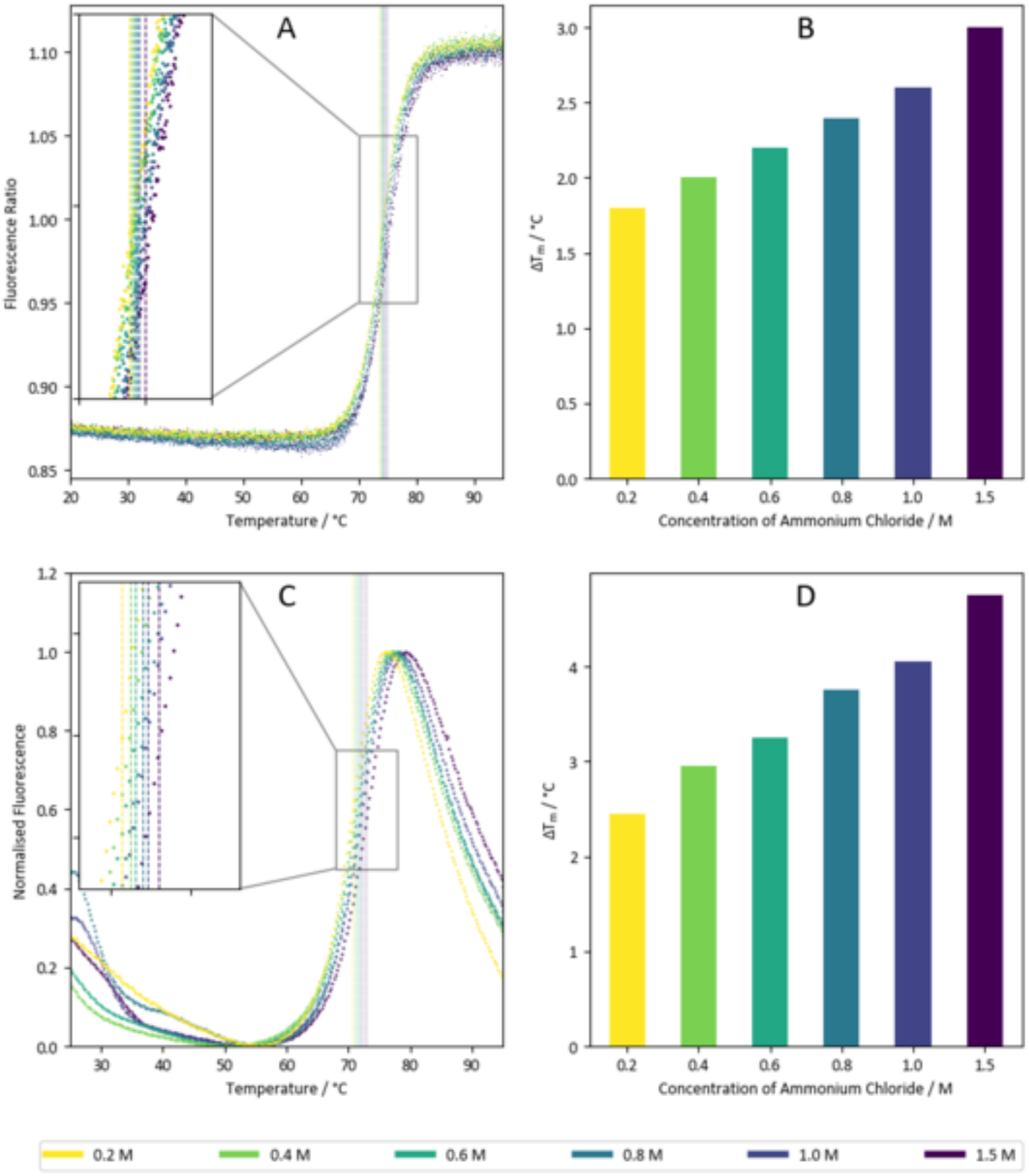

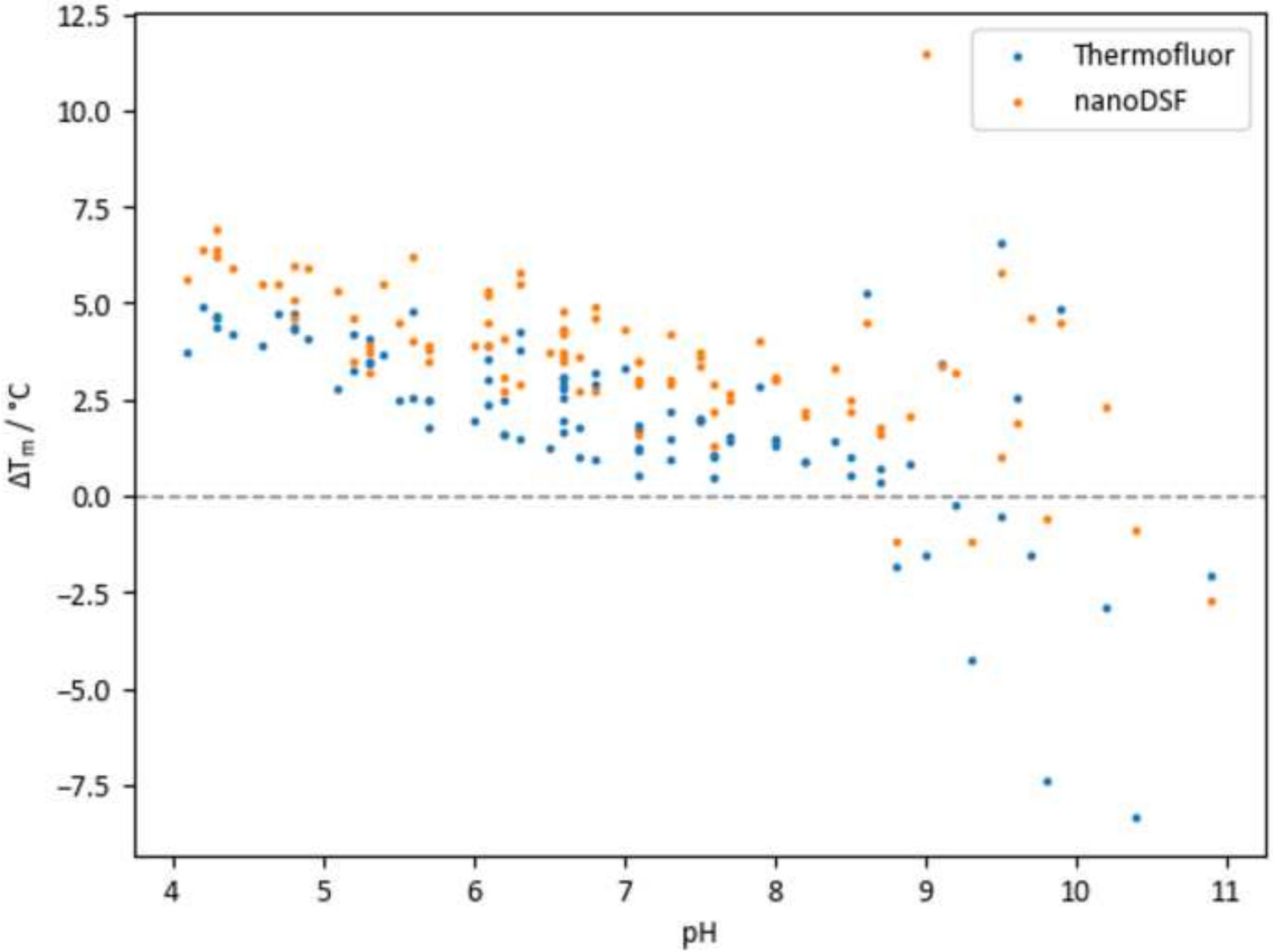

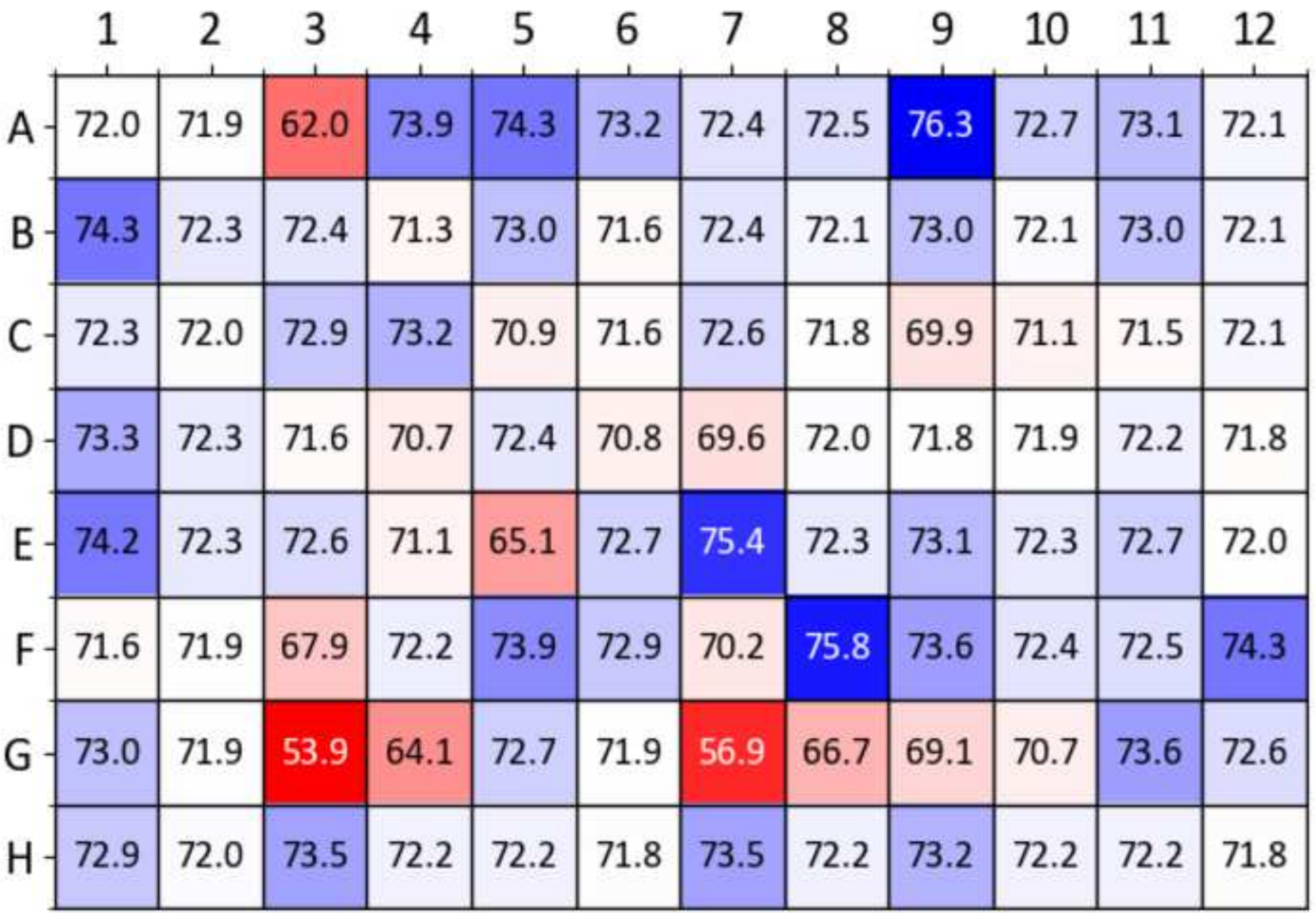

A

	1	2	3	4	5	6	7	8	9	10	11	12
A	70.8	70.8	64.1	74.0	74.0	72.4	71.2	70.8	73.9	71.4	69.4	70.8
B	71.3	70.9	71.2	70.4	71.6	70.5	71.0	70.9	72.7	71.3	71.7	70.8
C	71.1	70.9	71.3	70.3	71.1	69.7	71.8	71.9	70.6	70.2	69.8	66.6
D	–	69.4	70.7	69.8	63.3	70.0	70.3	70.6	71.0	70.7	71.0	70.5
E	73.2	71.1	70.5	70.3	58.6	57.1	43.1	70.9	69.3	70.9	64.4	69.6
F	69.6	70.5	41.2	67.6	68.7	64.6	46.3	52.2	68.9	69.8	68.3	70.0
G	69.3	70.6	58.2	43.2	70.7	70.6	41.6	45.5	64.0	69.4	68.5	69.5
H	69.0	70.2	66.8	69.5	71.2	70.8	69.6	70.4	71.1	70.8	59.1	63.5

B

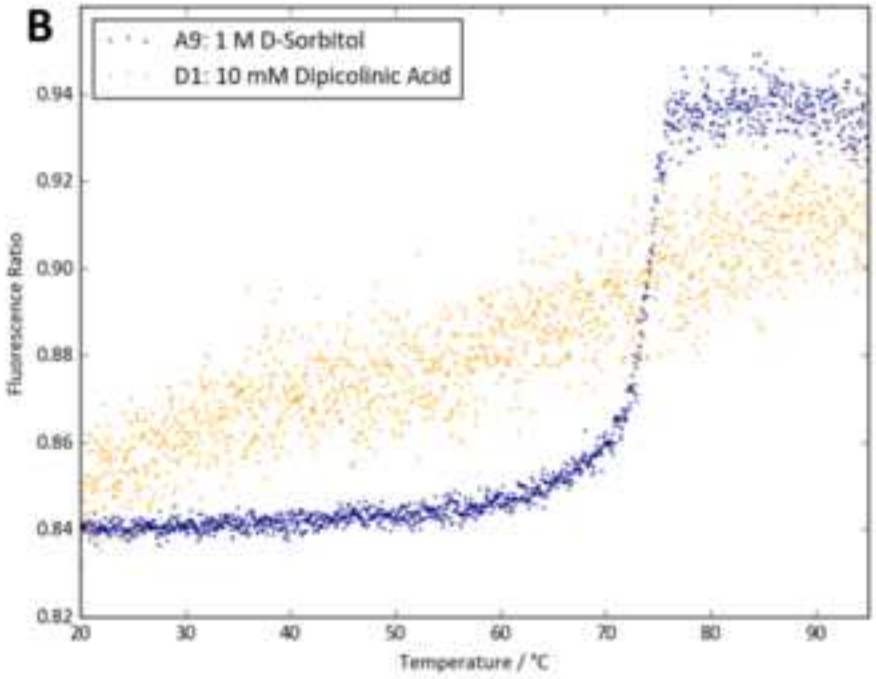

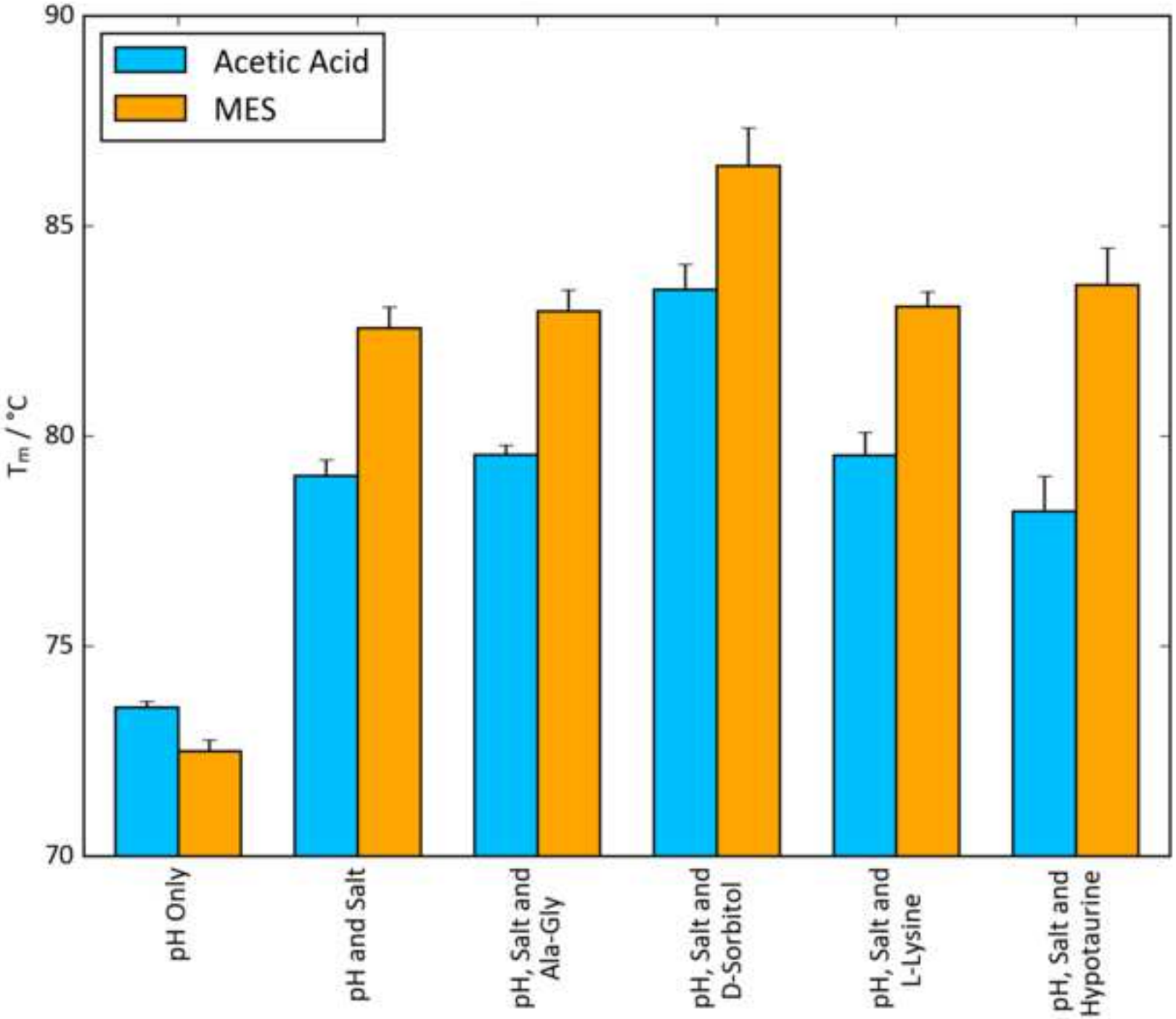

Name of Material/ Equipment	Company	Catalog Number	Comments/Description
Lysozyme	Melford Laboratories	L38100	Crystallised and lyophilised chicken egg white lysozyme.
The Durham pH Screen	Molecular Dimensions	MD1-101	96-well protein stability screen. See above for contents.
The Durham Salt Screen	Molecular Dimensions	MD1-102	96-well protein stability screen. See above for contents.
The Durham Osmolyte Screen	Various	#N/A	96-well protein stability screen, not commercially available at the time of publication. See above for contents.
SYPRO Orange	Invitrogen	S6651	Widely used fluorescent dye for protein staining in gels and DSF.
96-well PCR Plate	Starlab	1403-7700	Semi-skirted clear plastic for use with AB 7500 Fast RT-PCR System.
7500 Fast Real-time PCR System	Applied Biosystems	4362143	96-well format RT-PCR system. Alternative systems can be used. Analysis of data performed using free, open-access software NAMI. AB software tailored to DSF experiments using the 7500 Fast available at additional cost.
Prometheus NT.48	NanoTemper Technologies	#N/A	Label-free DSF system with up to 48-sample capacity. Can calculate unfolding temperatures (T_m and T_{onset}), critical denaturant concentrations (C_m), free folding energy (ΔG and ΔΔG), and aggregation results (T_{agg}) using built-in software.
Prometheus NT.48 Series nanoDSF Grade Standard Capillaries	NanoTemper Technologies	PR-C002	Prometheus NT.48 Series nanoDSF Grade Standard Capillaries. "High sensitivity" variants are available at a higher cost for use with low-concentration samples (<200 µg ml^{-1}).

jove JOURNAL OF VISUALIZED EXPERIMENTS
1 Alewife Center #200
Cambridge, MA 02140
tel. 617.945.9051
www.jove.com

ARTICLE AND VIDEO LICENSE AGREEMENT - UK

Title of Article: How to Stabilise Your Protein: Stability Screens for Thermal Shift Assays and nano Differential Scanning Fluorimetry for the Virus-X Project

Author(s): Daniel Bruce, Emily Cordew, Stefanie Freitag-Pohl, Ehmke Pohl

Item 1: The Author elects to have the Materials be made available (as described at http://www.jove.com/publish) via:

☐ Standard Access ☑ Open Access

Item 2: Please select one of the following items:

☑ The Author is **NOT** a United States government employee.

☐ The Author is a United States government employee and the Materials were prepared in the course of his or her duties as a United States government employee.

☐ The Author is a United States government employee but the Materials were NOT prepared in the course of his or her duties as a United States government employee.

ARTICLE AND VIDEO LICENSE AGREEMENT

1. **Defined Terms.** As used in this Article and Video License Agreement, the following terms shall have the following meanings: "**Agreement**" means this Article and Video License Agreement; "**Article**" means the article specified on the last page of this Agreement, including any associated materials such as texts, figures, tables, artwork, abstracts, or summaries contained therein; "**Author**" means the author who is a signatory to this Agreement; "**Collective Work**" means a work, such as a periodical issue, anthology or encyclopedia, in which the Materials in their entirety in unmodified form, along with a number of other contributions, constituting separate and independent works in themselves, are assembled into a collective whole; "**CRC License**" means the Creative Commons Attribution 3.0 Agreement (also known as CC-BY), the terms and conditions of which can be found at: http://creativecommons.org/licenses/by/3.0/us/legalcode ; "**Derivative Work**" means a work based upon the Materials or upon the Materials and other pre-existing works, such as a translation, musical arrangement, dramatization, fictionalization, motion picture version, sound recording, art reproduction, abridgment, condensation, or any other form in which the Materials may be recast, transformed, or adapted; "**Institution**" means the institution, listed on the last page of this Agreement, by which the Author was employed at the time of the creation of the Materials; "**JoVE**" means MyJove Corporation, a Massachusetts corporation and the publisher of The Journal of Visualized Experiments; "**Materials**" means the Article and / or the Video; "**Parties**" means the Author and JoVE; "**Video**" means any video(s) made by the Author, alone or in conjunction with any other parties, or by JoVE or its affiliates or agents, individually or in collaboration with the Author or any other parties, incorporating all or any portion of the Article, and in which the Author may or may not appear.

2. **Background.** The Author, who is the author of the Article, in order to ensure the dissemination and protection of the Article, desires to have the JoVE publish the Article and create and transmit videos based on the Article. In furtherance of such goals, the Parties desire to memorialize in this Agreement the respective rights of each Party in and to the Article and the Video.

3. **Grant of Rights in Article.** In consideration of JoVE agreeing to publish the Article, the Author hereby grants to JoVE, subject to **Sections 4 and 7** below, the exclusive, royalty-free, perpetual (for the full term of copyright in the Article, including any extensions thereto) license (a) to publish, reproduce, distribute, display and store the Article in all forms, formats and media whether now known or hereafter developed (including without limitation in print, digital and electronic form) throughout the world, (b) to translate the Article into other languages, create adaptations, summaries or extracts of the Article or other Derivative Works (including, without limitation, the Video) or Collective Works based on all or any portion of the Article and exercise all of the rights set forth in (a) above in such translations, adaptations, summaries, extracts, Derivative Works or Collective Works and (c) to license others to do any or all of the above. The foregoing rights may be exercised in all media and formats, whether now known or hereafter devised, and include the right to make such modifications as are technically necessary to exercise the rights in other media and formats. If the "Open Access" box has been checked in **Item 1** above, JoVE and the Author hereby grant to the public all such rights in the Article as provided in, but subject to all limitations and requirements set forth in, the CRC License.

jove JOURNAL OF VISUALIZED EXPERIMENTS
1 Alewife Center #200
Cambridge, MA 02140
tel. 617.945.9051
www.jove.com

ARTICLE AND VIDEO LICENSE AGREEMENT - UK

4. **Retention of Rights in Article.** Notwithstanding the exclusive license granted to JoVE in **Section 3** above, the Author shall, with respect to the Article, retain the non-exclusive right to use all or part of the Article for the non-commercial purpose of giving lectures, presentations or teaching classes, and to post a copy of the Article on the Institution's website or the Author's personal website, in each case provided that a link to the Article on the JoVE website is provided and notice of JoVE's copyright in the Article is included. All non-copyright intellectual property rights in and to the Article, such as patent rights, shall remain with the Author.

5. **Grant of Rights in Video - Standard Access.** This **Section 5** applies if the "Standard Access" box has been checked in **Item 1** above or if no box has been checked in **Item 1** above. In consideration of JoVE agreeing to produce, display or otherwise assist with the Video, the Author hereby acknowledges and agrees that, subject to **Section 7** below, JoVE is and shall be the sole and exclusive owner of all rights of any nature, including, without limitation, all copyrights, in and to the Video. To the extent that, by law, the Author is deemed, now or at any time in the future, to have any rights of any nature in or to the Video, the Author hereby disclaims all such rights and transfers all such rights to JoVE.

6. **Grant of Rights in Video - Open Access.** This **Section 6** applies only if the "Open Access" box has been checked in **Item 1** above. In consideration of JoVE agreeing to produce, display or otherwise assist with the Video, the Author hereby grants to JoVE, subject to **Section 7** below, the exclusive, royalty-free, perpetual (for the full term of copyright in the Article, including any extensions thereto) license (a) to publish, reproduce, distribute, display and store the Video in all forms, formats and media whether now known or hereafter developed (including without limitation in print, digital and electronic form) throughout the world, (b) to translate the Video into other languages, create adaptations, summaries or extracts of the Video or other Derivative Works or Collective Works based on all or any portion of the Video and exercise all of the rights set forth in (a) above in such translations, adaptations, summaries, extracts, Derivative Works or Collective Works and (c) to license others to do any or all of the above. The foregoing rights may be exercised in all media and formats, whether now known or hereafter devised, and include the right to make such modifications as are technically necessary to exercise the rights in other media and formats.

7. **Government Employees.** If the Author is a United States government employee and the Article was prepared in the course of his or her duties as a United States government employee, as indicated in **Item 2** above, and any of the licenses or grants granted by the Author hereunder exceed the scope of the 17 U.S.C. 403, then the rights granted hereunder shall be limited to the maximum rights permitted under such statute. In such case, all provisions contained herein that are not in conflict with such statute shall remain in full force and effect, and all provisions contained herein that do so conflict shall be deemed to be amended so as to provide to JoVE the maximum rights permissible within such statute.

8. **Protection of the work.** The Author(s) authorize JoVE to take steps in the Author(s) name and on their behalf if JoVE believes some third party could be infringing or might infringe the copyright of either the Author's Article and/or Video.

9. **Likeness, Privacy, Personality.** The Author hereby grants JoVE the right to use the Author's name, voice, likeness, picture, photograph, image, biography and performance in any way, commercial or otherwise, in connection with the Materials and the sale, promotion and distribution thereof. The Author hereby waives any and all rights he or she may have, relating to his or her appearance in the Video or otherwise relating to the Materials, under all applicable privacy, likeness, personality or similar laws.

10. **Author Warranties**. The Author represents and warrants that the Article is original, that it has not been published, that the copyright interest is owned by the Author (or, if more than one author is listed at the beginning of this Agreement, by such authors collectively) and has not been assigned, licensed, or otherwise transferred to any other party. The Author represents and warrants that the author(s) listed at the top of this Agreement are the only authors of the Materials. If more than one author is listed at the top of this Agreement and if any such author has not entered into a separate Article and Video License Agreement with JoVE relating to the Materials, the Author represents and warrants that the Author has been authorized by each of the other such authors to execute this Agreement on his or her behalf and to bind him or her with respect to the terms of this Agreement as if each of them had been a party hereto as an Author. The Author warrants that the use, reproduction, distribution, public or private performance or display, and/or modification of all or any portion of the Materials does not and will not violate, infringe and/or misappropriate the patent, trademark, intellectual property or other rights of any third party. The Author represents and warrants that it has and will continue to comply with all government, institutional and other regulations, including, without limitation all institutional, laboratory, hospital, ethical, human and animal treatment, privacy, and all other rules, regulations, laws, procedures or guidelines, applicable to the Materials, and that all research involving human and animal subjects has been approved by the Author's relevant institutional review board.

11. **JoVE Discretion.** If the Author requests the assistance of JoVE in producing the Video in the Author's facility, the Author shall ensure that the presence of JoVE employees, agents or independent contractors is in accordance with the relevant regulations of the Author's institution. If more than one author is listed at the beginning of this Agreement, JoVE may, in its sole discretion, elect not take any action with respect to the Article until such time as it has received complete, executed Article and Video License Agreements from each such author. JoVE reserves the right, in its absolute and sole

jove JOURNAL OF VISUALIZED EXPERIMENTS
1 Alewife Center #200
Cambridge MA 02140
tel. 617.945.9051
www.jove.com

ARTICLE AND VIDEO LICENSE AGREEMENT - UK

discretion andwithout giving any reason therefore, to accept or decline any work submitted to JoVE. JoVE and its employees, agents and independent contractors shall have full, unfettered access to the facilities of the Author or of the Author's institution as necessary to make the Video, whether actually published or not. JoVE has sole discretion as to the method of making and publishing the Materials, including, without limitation, to all decisions regarding editing, lighting, filming, timing of publication, if any, length, quality, content and the like.

12. **Indemnification.** The Author agrees to indemnify JoVE and/or its successors and assigns from and against any and all claims, costs, and expenses, including attorney's fees, arising out of any breach of any warranty or other representations contained herein. The Author further agrees to indemnify and hold harmless JoVE from and against any and all claims, costs, and expenses, including attorney's fees, resulting from the breach by the Author of any representation or warranty contained herein or from allegations or instances of violation of intellectual property rights, damage to the Author's or the Author's institution's facilities, fraud, libel, defamation, research, equipment, experiments, property damage, personal injury, violations of institutional, laboratory, hospital, ethical, human and animal treatment, privacy or other rules, regulations, laws, procedures or guidelines, liabilities and other losses or damages related in any way to the submission of work to JoVE, making of videos by JoVE, or publication in JoVE or elsewhere by JoVE. The Author shall be responsible for, and shall hold JoVE harmless from, damages caused by lack of sterilization, lack of cleanliness or by contaminationdue to the making of a video by JoVE its employees, agents or independent contractors. All sterilization, cleanliness or decontamination procedures shall be solely the responsibility of the Author and shall be undertaken at the Author's expense. All indemnifications provided herein shall include JoVE's attorney's fees and costs related to said losses or damages. Such indemnification and holding harmless shall include such losses or damages incurred by, or in connection with, acts or omissions of JoVE, its employees, agents or independent contractors.

13. **Fees.** To cover the cost incurred for publication, JoVE must receive payment before production and publication of the Materials. Payment is due in 21 days of invoice. Should the Materials not be published due to an editorial or production decision, these funds will be returned to the Author. Withdrawal by the Author of any submitted Materials after final peer review approval will result in a US$1,200 fee to cover pre-production expenses incurred by JoVE. If payment is not received by the completion of filming, production and publication of the Materials will be suspended until payment is received.

14. **Transfer, Governing Law.** This Agreement may be assigned by JoVE and shall inure to the benefits of any of JoVE's successors and assignees. This Agreement shall be governed and construed by the internal laws of the Commonwealth of Massachusetts without giving effect to any conflict of law provision thereunder. This Agreement may be executed in counterparts, each of which shall be deemed an original, but all of which together shall be deemed to me one and the same agreement. A signed copy of this Agreement delivered by facsimile, e-mail or other means of electronic transmission shall be deemed to have the same legal effect as delivery of an original signed copy of this Agreement.

A signed copy of this document must be sent with all new submissions. Only one Agreement is required per submission.

CORRESPONDING AUTHOR

Name:	Ehmke Pohl
Department:	Chemistry
Institution:	Durham University
Title:	Reader
Signature:	Ehmke Pohl
Date:	13. 8. 2018

Please submit a **signed** and **dated** copy of this license by one of the following three methods:

1. Upload an electronic version on the JoVE submission site
2. Fax the document to +1.866.381.2236
3. Mail the document to JoVE / Attn: JoVE Editorial / 1 Alewife Center #200 / Cambridge, MA 02140

Dr. Ehmke Pohl
Reader in Protein Crystallography
Co-Director Biophysical Sciences Institute
Direct Line: 0191 334 3619
Email: ehmke.pohl@durham.ac.uk

To the editor of *JoVE*

Dear Madam/Sir

Thank you very much for accepting our revised manuscript entitled "How to Stabilise your Protein: Stability Screens for Thermal Shift Assays and nano Differential Scanning Fluorimetry in the Virus-X Project" by Daniel Bruce *et al*. for publication.

We have amended the paper according to your comments, changed the figures as requested and add the missing grant codes.

With best regards,

Ehmke Pohl

Department of Chemistry and Department of Biosciences
Science Site, South Road, Durham. DH1 3LE

Supplementary Information: Composition of Stability Screens

All concentrations recorded are working concentrations (i.e. diluted two-fold for use in an assay). Actual screen concentrations as sold are twice as much as reported values.

Supplementary Table 1 Salt Screen

Supplementary Table 2 pH Screen

Supplementary Table 3 Osmolyte Screen

	1	2	3	4	5	6	7	8
A	water	water	4 M urea	3.0 M Gu-HCl	1.0 M Gu-HCl	0.8 M Gu-HCl	0.6 M Gu-HCl	0.4 M Gu-HCl
B	1.5 M Na_2 malonate	1.0 M Na_2 malonate	0.8 M Na_2 malonate	0.6 M Na_2 malonate	0.4 M Na_2 malonate	0.2 M Na_2 malonate	1.5 M $(NH_4)_2SO_4$	1.0 M $(NH_4)_2SO_4$
C	1.5 M NaCl	1.0 M NaCl	0.8 M NaCl	0.6 M NaCl	0.4 M NaCl	0.2 M NaCl	1.5 M NH_4Cl	1.0 M NH_4Cl
D	1.0 M $MgSO_4$	0.8 M $MgSO_4$	0.6 M $MgSO_4$	0.4 M $MgSO_4$	0.2 M $MgSO_4$	1.0 M Na_2SO_4	0.8 M Na_2SO_4	0.6 M Na_2SO_4
E	0.5 M LiCl	0.2 M LiCl	0.5 M RbCl	0.2 M RbCl	0.5 M CsCl	0.2 M CsCl	0.4 M NaF	0.1 M NaF
F	0.1 M NaI	0.4 M $MgCl_2$	5 mM $MgCl_2$	5 mM $CaCl_2$	5 mM $SrCl_2$	1 mM $ZnCl_2$	0.1 mM $ZnCl_2$	1 mM $NiCl_2$
G	0.1 mM $CoCl_2$	1 mM $CuSO_4$	0.1 mM CuSO4	1 mM $CdSO_4$	5 mM EDTA pH 7.5	5 mM EGTA pH 7.5	2 mM magic triangle pH 7.0	2 mM $La(NO_3)_3$
H	2 mM $GdCl_3$	2 mM $DyCl_3$	2 mM $HoCl_3$	2 mM $YbCl_3$	2 mM $LuCl_3$	5 mM Na_2HPO_4	5 mM Na_3VO_4	5 mM Na_2WO_4

9	10	11	12
0.2 M Gu-HCl	5 mM Gu-HCl	0.5 M Na_3 citrate	0.2 M Na_3 citrate
0.8 M $(NH_4)_2SO_4$	0.6 M $(NH_4)_2SO_4$	0.4 M $(NH_4)_2SO_4$	0.2 M $(NH_4)_2SO_4$
0.8 M NH_4Cl	0.6 M NH_4Cl	0.4 M NH_4Cl	0.2 M NH_4Cl
0.4 M Na_2SO_4	0.2 M Na_2SO_4	0.5 M KCl	0.2 M KCl
1.5 M NaBr	0.4 M NaBr	0.1 M NaBr	0.4 M NaI
0.1 mM $NiCl_2$	5 mM $MnCl_2$	0.5 mM $MnCl_2$	1 mM $CoCl_2$
2 mM $PrCl_3$	2 mM $NdCl_3$	2 mM $SmCl_3$	2 mM $EuCl_3$
5 mM Na_2MoO_4	5 mM DTT	5 mM TCEP pH 7.0	5 mM β-mercapto ethanol

	1	2	3	4	5	6	7	8
A	water	water	4 M urea	100 mM citric acid pH 4.1	100 mM citric acid pH 4.6	100 mM citric acid pH 5.1	100 mM acetic acid pH 4.2	100 mM acetic acid pH 4.7
B	100 mM malic acid pH 4.3	100 mM malic acid pH 4.8	100 mM malic acid pH 5.3	100 mM tartaric acid pH 4.3	100 mM tartaric acid pH 4.8	100 mM tartaric acid pH 5.3	100 mM propionic acid pH 4.3	100 mM propionic acid pH 4.8
C	100 mM citric acid pH 5.5	100 mM citric acid pH 6.0	100 mM citric acid pH 6.5	100 mM succinic acid pH 5.6	100 mM succinic acid pH 6.1	100 mM succinic acid pH 6.6	100 mM MES pH 5.6	100 mM MES pH 6.1
D	100 mM sodium cacodylate pH 5.7	100 mM sodium cacodylate pH 6.2	100 mM sodium cacodylate pH 6.7	100 mM ADA pH 6.1	100 mM ADA pH 6.6	100 mM ADA pH 7.1	100 mM bisTRIS pH 6.1	100 mM bisTRIS pH 6.6
E	100 mM phosphate pH 6.3	100 mM phosphate pH 6.8	100 mM phosphate pH 7.3	100 mM PIPES pH 6.3	100 mM PIPES pH 6.8	100 mM PIPES pH 7.3	100 mM imidazole pH 6.6	100 mM imidazole pH 7.1
F	100 mM bisTRIS propane pH 6.6	100 mM bisTRIS propane pH 7.1	100 mM bisTRIS propane pH 7.6	100 mM HEPES pH 7.0	100 mM HEPES pH 7.5	100 mM HEPES pH 8.0	100 mM tricine pH 7.5	100 mM tricine pH 8.0
G	100 mM TRIS pH 7.7	100 mM TRIS pH 8.2	100 mM TRIS pH 8.7	100 mM bicine pH 7.7	100 mM bicine pH 8.2	100 mM bicine pH 8.7	100 mM TAPS pH 7.9	100 mM TAPS pH 8.4
H	100 mM boric acid pH 8.6	100 mM boric acid pH 9.1	100 mM boric acid pH 9.6	100 mM CHES pH 8.8	100 mM CHES pH 9.3	100 mM CHES pH 9.8	100 mM glycine pH 9.2	100 mM glycine pH 9.7

9	10	11	12
100 mM acetic acid pH 5.2	100 mM succinic acid pH 4.4	100 mM succinic acid pH 4.9	100 mM succinic acid pH 5.4
100 mM propionic acid pH 5.3	100 mM malonic acid pH 5.2	100 mM malonic acid pH 5.7	100 mM malonic acid pH 6.2
100 mM MES pH 6.6	100 mM maleic acid pH 5.7	100 mM maleic acid pH 6.2	100 mM maleic acid pH 6.7
100 mM bisTRIS pH 7.1	100 mM ACES pH 6.3	100 mM ACES pH 6.8	100 mM ACES pH 7.3
100 mM imidazole pH 7.6	100 mM MOPS pH 6.6	100 mM MOPS pH 7.1	100 mM MOPS pH 7.6
100 mM tricine pH 8.5	100 mM EPPS pH 7.5	100 mM EPPS pH 8.0	100 mM EPPS pH 8.5
100 mM TAPS pH 8.9	100 mM bisTRIS propane pH 8.5	100 mM bisTRIS propane pH 9.0	100 mM bisTRIS propane pH 9.5
100 mM glycine pH 10.2	100 mM CAPS pH 9.9	100 mM CAPS pH 10.4	100 mM CAPS pH 10.9

	1	2	3	4	5	6	7	8
A	water	water	4 M urea	30% glycerol	20% glycerol	10% glycerol	160 mM xylitol	20 mM xylitol
B	500 mM D-sucrose	50 mM D-sucrose	250 mM D-galactose	25 mM D-galactose	500 mM D-glucose	50 mM D-glucose	65 mM D-trehalose	10 mM D-trehalose
C	70 mM maltitol	10 mM maltitol	250 mM D-mannitol	25 mM D-mannitol	200 mM NDSB-195	200 mM NDSB-201	200 mM NDSB-211	200 mM NDSB-221
D	10 mM dipicolinic acid	2 mM dipicolinic acid	1 mM spermidine	1 mM spermine HCl	250 mM methyl butyrate	20 mM methyl butyrate	250 mM sodium butyrate	20 mM sodium butyrate
E	750 mM TMAO	100 mM TMAO	100 mM sarcosine	10 mM sarcosine	100 mM carnitine	10 mM carnitine	100 mM hypotaurine	10 mM hypotaurine
F	100 mM choline	10 mM choline	25 mM glyphosate	3 mM glyphosate	100 mM Ala-Ala	10 mM Ala-Ala	100 mM Ala-Gly	10 mM Ala-Gly
G	120 mM L-glutamic acid	15 mM L-glutamic acid	200 mM L-glutamine	50 mM L-glutamine	200 mM L-proline	50 mM L-proline	200 mM 5-oxoproline	50 mM 5-oxoproline
H	140 mM L-citrulline	30 mM L-citrulline	200 mM glycine	50 mM glycine	200 mM trimethyl glycine	50 mM trimethyl glycine	200 mM L-alanine	50 mM L-alanine

9	10	11	12
1 mM D-sorbitol	200 mM D-sorbitol	250 mM D-maltose	25 mM D-maltose
1 M L-arabinose	200 mM L-arabinose	135 mM myo-inositol	15 mM myo-inositol
100 mM NDSB-256	50 mM pyridine	50 mM pyrimidine	2 mM adenine
100 mM ectoine	10 mM ectoine	100 mM hydroxy ectoine	10 mM hydroxy ectoine
100 mM taurine	10 mM taurine	100 mM acetylcholine	10 mM acetylcholine
100 mM Ala-Leu	10 mM Ala-Leu	100 mM Gly-Gly	10 mM Gly-Gly
125 mM L-arginine	25 mM L-arginine	200 mM L-lysine HCl	50 mM L-lysine HCl
200 mM β-alanine	50 mM β-alanine	60 mM L-histidine	15 mM L-histidine